CHAPTER 4

RESULTS AND DISCUSSIONS

4.1 Introduction

In this chapter, the experimental results for fluid flow inside straight micro-diameter tubes and helical coil sections prepared from these tubes are presented. Heat transfer characteristics of a helical coil are also discussed. Effort has been made to develop a generalized correlation for helical coils. The experimentally obtained friction factor and Nusselt number data are also compared with empirical correlations available in the literature.

4.2 Flow characteristics

In order to test the accuracy of experimental setup pressure drop data were taken on straight tubes of all diameter used for making helical coils. The experiments were conducted for single phase laminar flow inside straight sections of micro-diameter tubes and their helical coil sections. After taking observation on straight micro-diameter tube the same was wound round on a cylindrical frame of known diameter to form a helical coil. Three straight tubes and their coils are used in the present study to examine the hydrodynamic behaviour using water, methanol, and acetone as working fluids. Variation of pressure drop with flow rate in straight micro-diameter tube and their helical coil sections for all working fluids and friction factor-Reynolds number data are discussed in following subsections.

4.2.1. Flow through straight tubes

Effect of flow rate on pressure drop in straight tube section was investigated with three smooth tubes of inner diameter 720, 850 and 1000 μm. These results are shown as ΔP vs u plots in Figures 4.1 to 4.3 for each tube and for all three fluids. From the shape of plots it can be seen that the experimental data satisfy general

relation $\Delta P \alpha u^2$. These figures represent effect of fluid on pressure drop for straight micro-diameter tubes of different inner diameters for the three working fluids used in this work. Pressure drop values in case of water are higher as compared to those for methanol and acetone due to its viscous nature. Viscosity of water is more than that of methanol and acetone. Acetone is a less viscous fluid that is why it has lower pressure drop. Methanol also offers very lower pressure drop than water but higher than acetone.

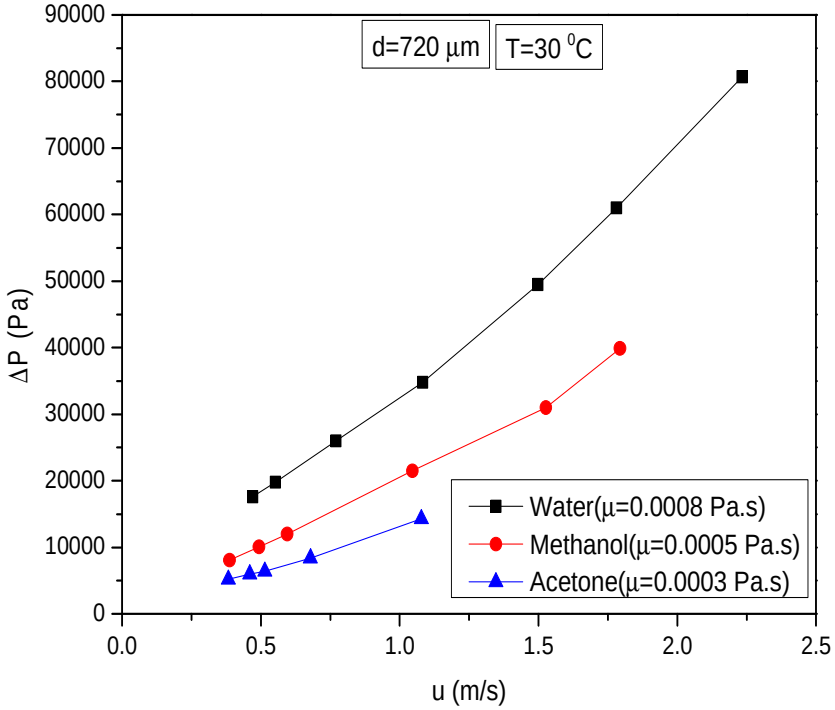

Fig.4.1 Pressure drop vs. velocity in a straight tube of inner diameter 720 μm for all three fluids

These figures also show the effect of tube diameter on pressure drop inside straight micro-diameter tubes. From these figures it can be easily observed that as expected tube diameter has significant effect on pressure drop. As the tube diameter decreases pressure drop increases. Pressure drop is inversely proportional to tube diameter.

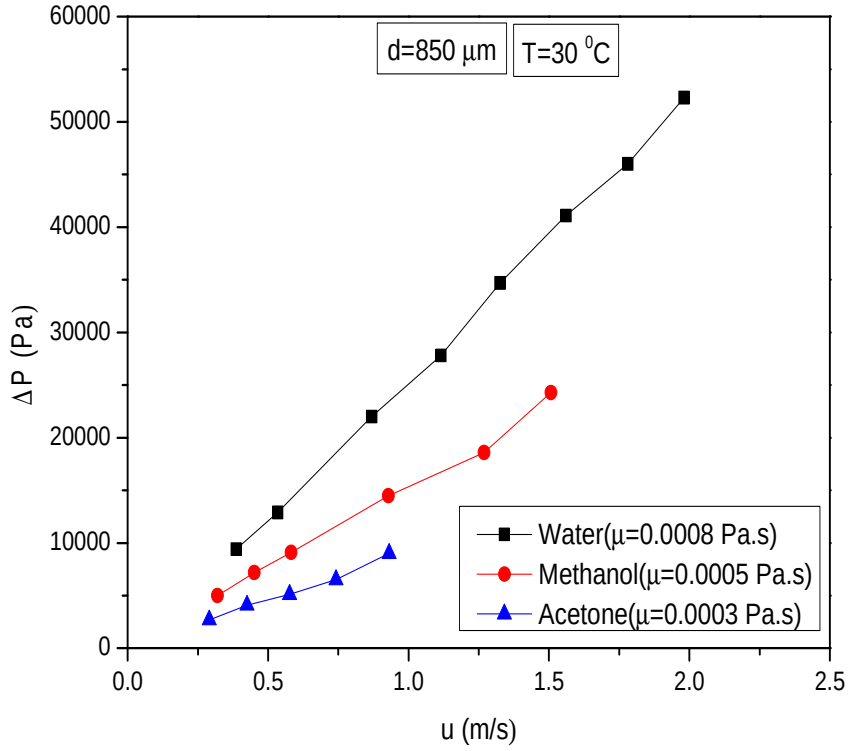

Fig.4.2 Pressure drop vs. velocity in a straight tube of inner diameter 850 μm for all three fluids

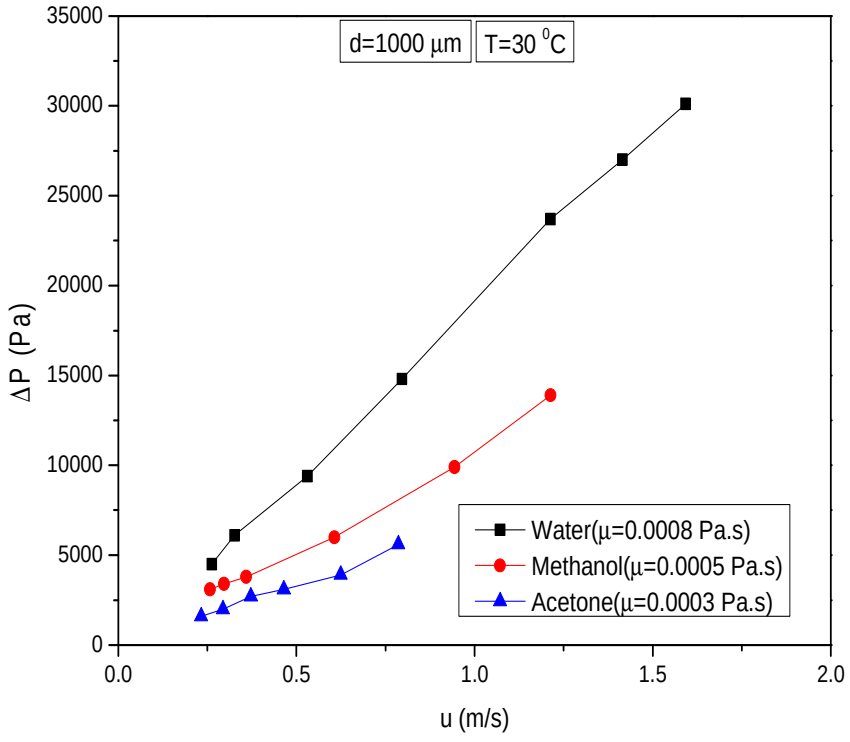

Fig.4.3 Pressure drop vs. velocity in a straight tube of inner diameter 1000 μm for all three fluids

4.2.2 Flow through helical coil sections

To study the effect of flow rate on pressure drop in helical coil section experiments were performed separately with coils made from three tubes of inner diameter 720, 850 and 1000 μm using water, methanol, and acetone as working fluids. The results are shown in Figures 4.4 to 4.6 as ΔP vs u plots. These results follow similar behaviour as observed and discussed in Section 4.2.1 for straight tubes. Here it is noticeable that the pressure drop in helical coil sections is comparatively higher than those for the straight micro-diameter tubes of the same diameter and length. Due to curved nature secondary flow sets in helical coil hence pressure drop at given flow rate is greater than that in a straight tube of the same diameter.

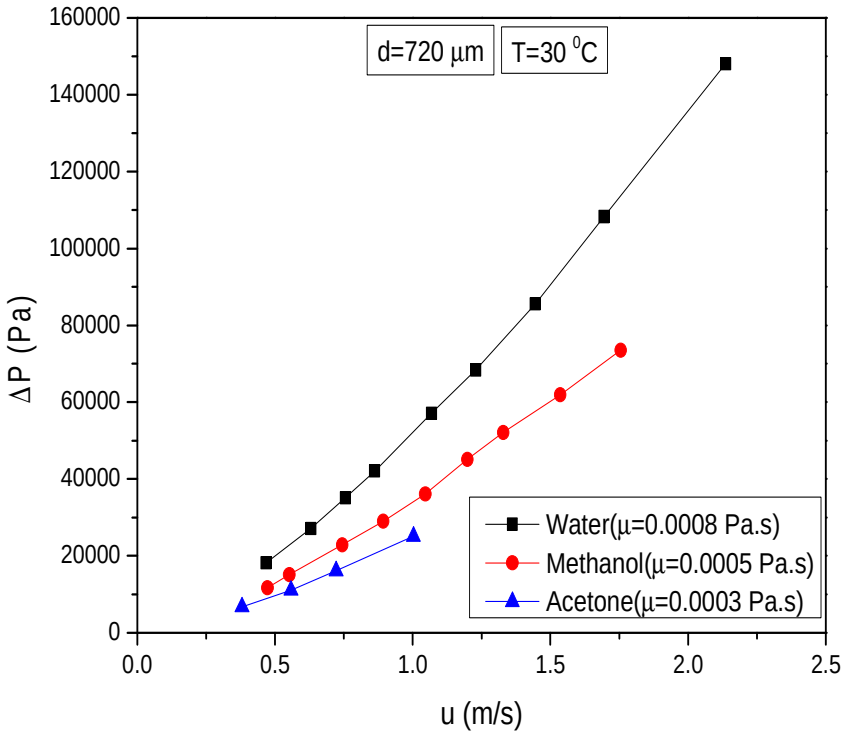

Fig.4.4 Pressure drop vs. velocity in a helical coil of inner tube diameter 720 μm for all three fluids

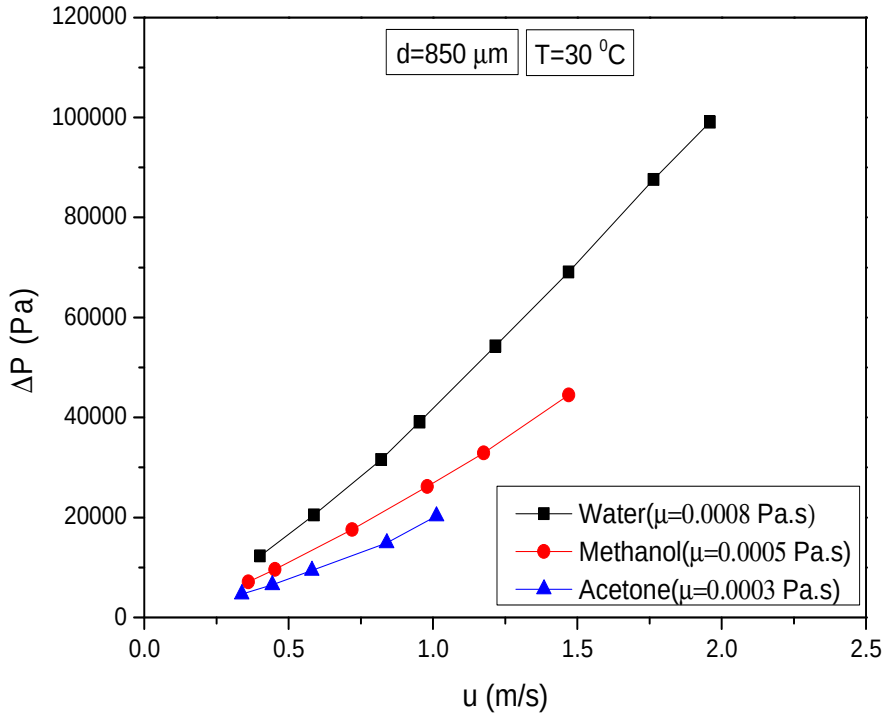

Fig.4.5 Pressure drop vs. velocity in a helical coil of inner tube diameter 850 μm for all three fluids

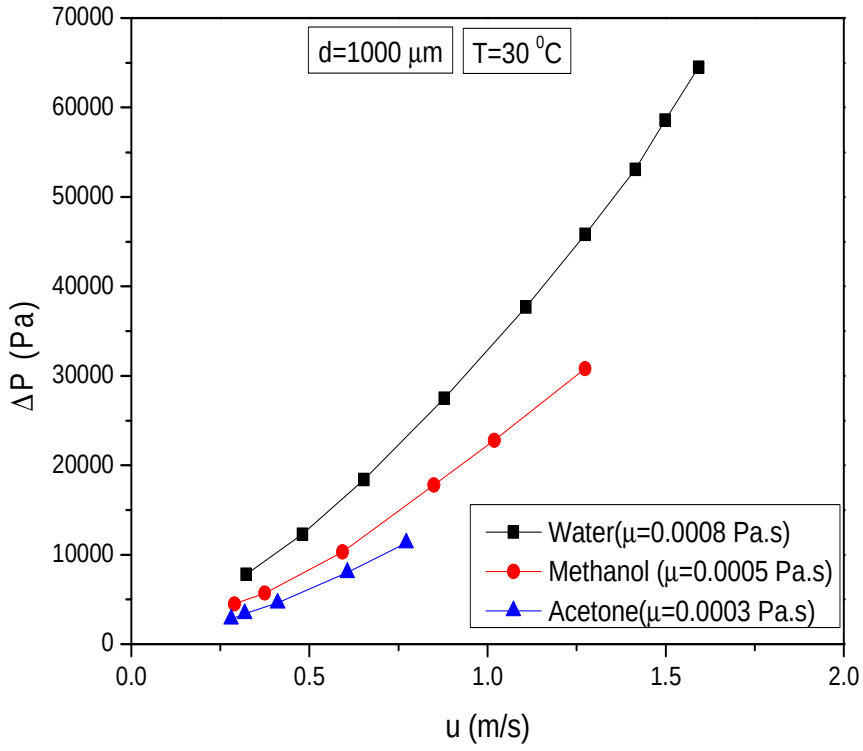

Fig.4.6 Pressure drop vs. velocity in a helical coil of inner tube diameter 1000 μm for all three fluids

4.2.3 Variation of friction factor with Reynolds number

Variation of friction factor with Reynolds number in straight micro-diameter tube sections and helical coil sections for the three working fluids are shown in Figures 4.7 to 4.9. The setup was first calibrated by obtaining the friction factor data on straight tubes. These results are discussed as f vs Re plots. The Reynolds number has varied from 409 to 2096 in straight micro-diameter tubes and 401 to 2073 in helical coils respectively. The friction factor data of all straight micro-diameter tubes and helical coils for all working fluids are presented in Table D.3 and D.4. Experimentally obtained friction factor are also compared with relation $f = 16/\mathrm{Re}$. The friction factor results are found to be in excellent agreement with the laminar flow equation for smooth straight tubes. It is seen that experimental values are in close agreement with theoretical relation. The deviations are being within ± 5 % (i.e. well within the experimental errors).

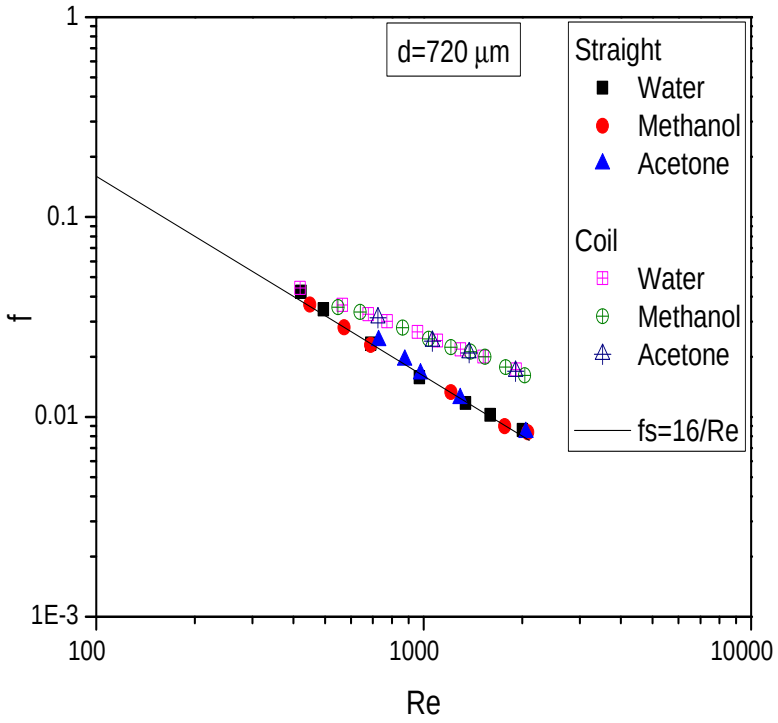

Fig.4.7 Variation of friction factor with Reynolds number in straight tube and helical coil of inner tube diameter 720 μm for all three working fluids

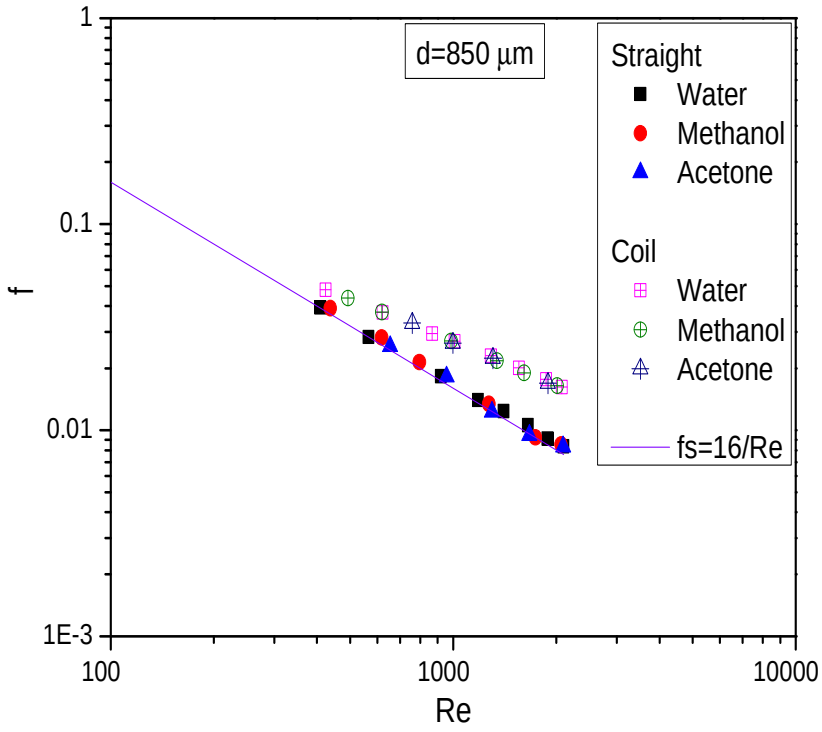

Fig.4.8 Variation of friction factor with Reynolds number in straight tube and helical coil of inner tube diameter 850 μm for all three working fluids

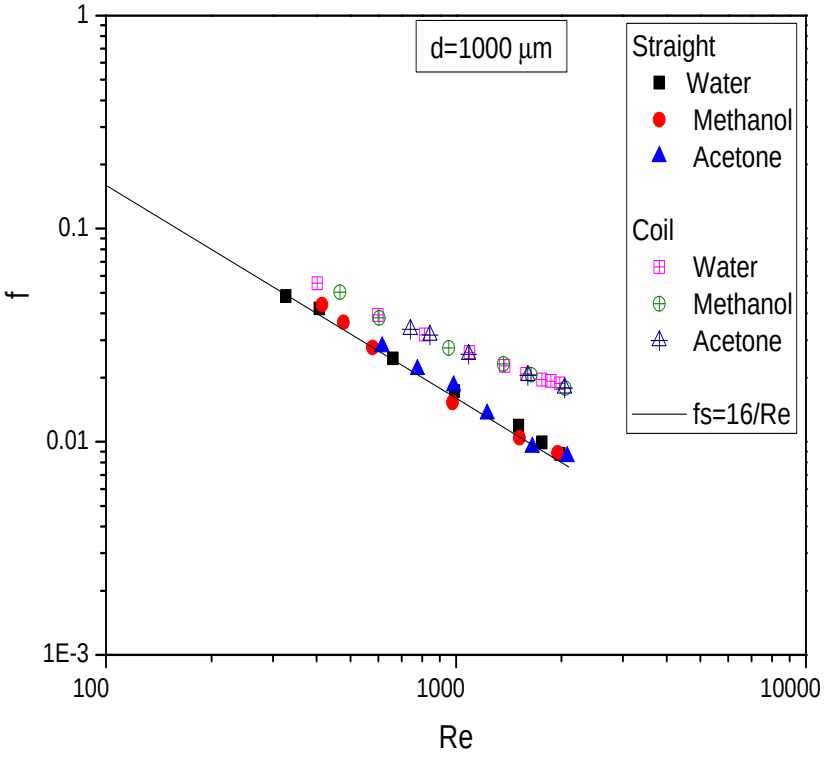

Fig.4.9 Variation of friction factor with Reynolds number in straight tube and helical coil of inner tube diameter 1000 μm for all three working fluids

From these figures it is observed that friction factor decreases as Reynolds number increases. As expected, the values obtained for friction factor, helical coils, are comparatively higher than those of the straight tube. At very low Reynolds number, velocity being small, fluid elements remains blind to the curvature and the viscous forces dominate the centrifugal forces. As the flow rate increases, centrifugal force becomes of considerable magnitude and thus inertia force in the fluid has to overcome the effect of both the viscous and centrifugal forces. The difference between friction factors for the helical coil and the straight micro-diameter tube is small at low Re compared to that at high Re. This can be attributed to intensity of secondary flow at high flow rates.

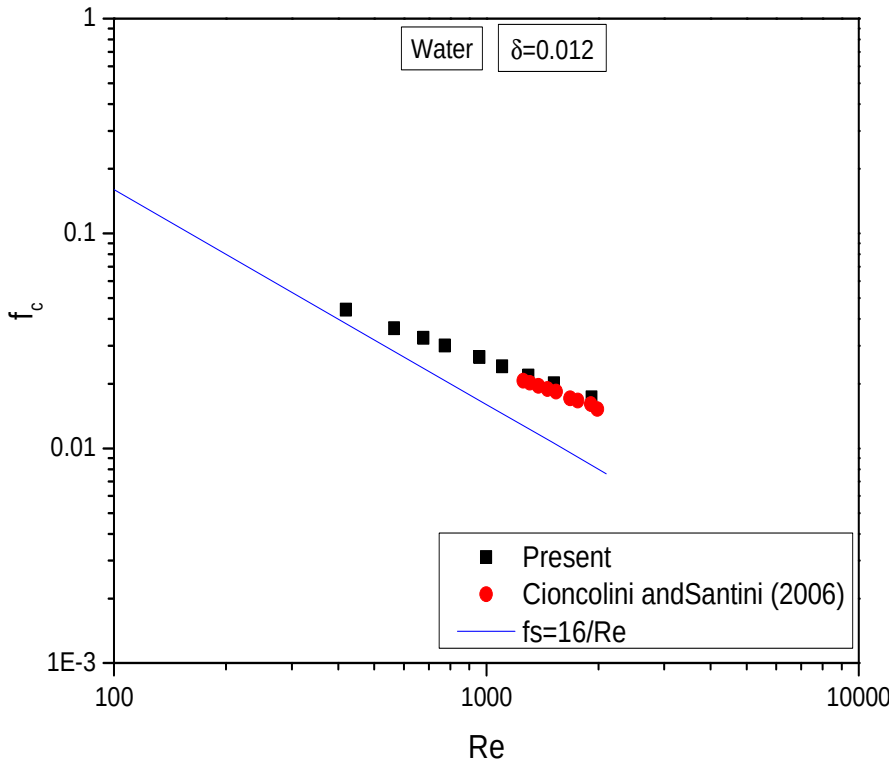

Fig.4.10 Present and Cioncolini and Santini's (2006) experimental friction factor data in helical coil of curvature ratio 0.012

Figure 4.10 shows the friction factor data of present and Cioncolini and Santini (2006) in helical coil of curvature ratio 0.012 using water as working fluid. Cioncolini and Santini's (2006) friction factor data (Table D.9) was generated from conventional tube of d=8.59 mm, D=729.5 mm and p=22 mm. However, present friction factor data was generated from helical coil of micro-diameter tube of 720 μm.

4.2.4 Variation of friction factor with Dean number in helical coils

Variation of friction factor with Dean number in helical coils of different curvature ratio is shown in Figures 4.11 to 4.13. The line representing values predicted from the correlation of Srinivasan et al. (1968).The Dean number has varied from 45 to 270. These figures show values comparison between experimentally obtained friction factors with values predicted from the correlation of Srinivasan et al. (1968) (eqn. 2.49) for helically coil for all working fluids under laminar flow conditions. From these figures it is observed that predicted values are consistently lower than the experimental values by 15 %. Srinivasan et al.'s (1968) correlation was developed over a different range of Dean number valid for curvature ratios of $0.0097 < d/D < 0.135$ using water as working fluid. From these figures it is also observed that friction factor decreases as Dean number increases.

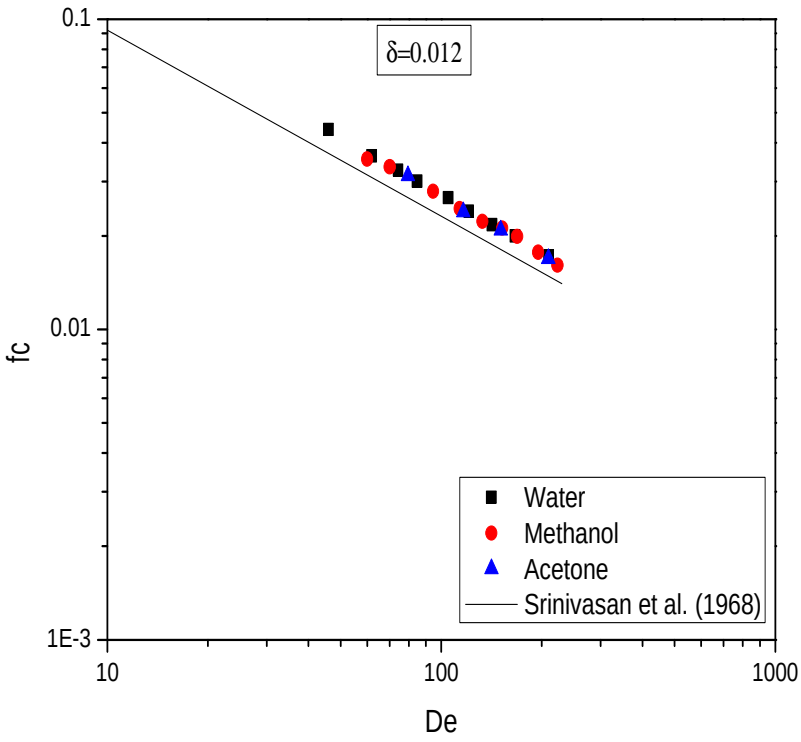

Fig.4.11 Variation of friction factor with Dean number in a helical coil of curvature ratio 0.012

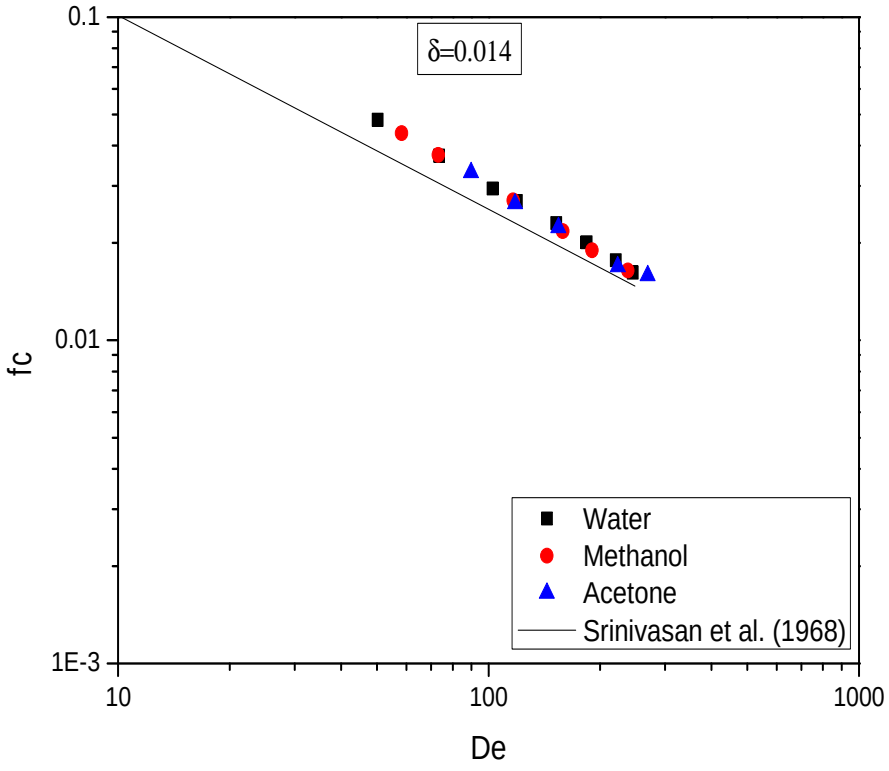

Fig.4.12 Variation of friction factor with Dean number in a helical coil of curvature ratio 0.014

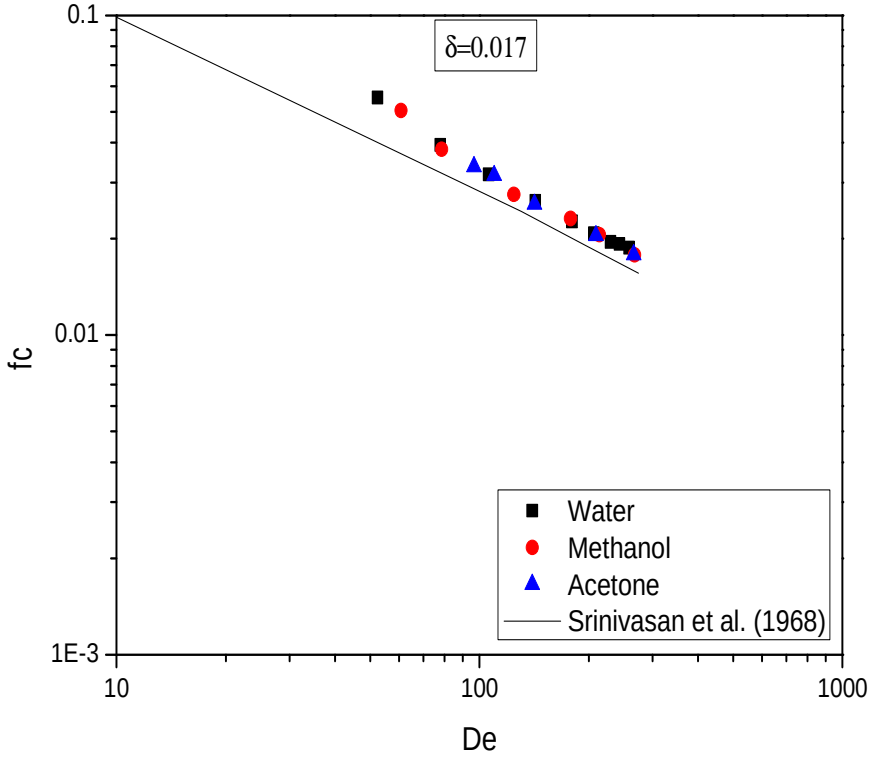

Fig.4.13 Variation of friction factor with Dean number in a helical coil of curvature ratio 0.017

4.2.5 Correlation for friction factor

The laminar flow friction factor data of three coils having constant coil diameter and pitch are generated in the present study. The least squares regression analysis has been used to develop an empirical correlation:

$$\frac{f_c}{f_s} = 1 + 0.005De \tag{4.1}$$

The above correlation is valid for the range $\delta = 0.012 - 0.017$ and $45 < De < 270$ and correlates present data with a standard deviation of $\pm 5\%$.

From above equation it is noticeable that for laminar flow if Dean number is low, helical coil behave as a hydrodynamically straight tube. Hence $De = 0$, results $f_c = f_s$ helical coil behave as a straight tube.

The f_c / f_s ratio predicted from present correlation is plotted against experimental f_c / f_s values as shown in Figure 4.14. It is observed that most of the data lie within $\pm 5\%$ band.

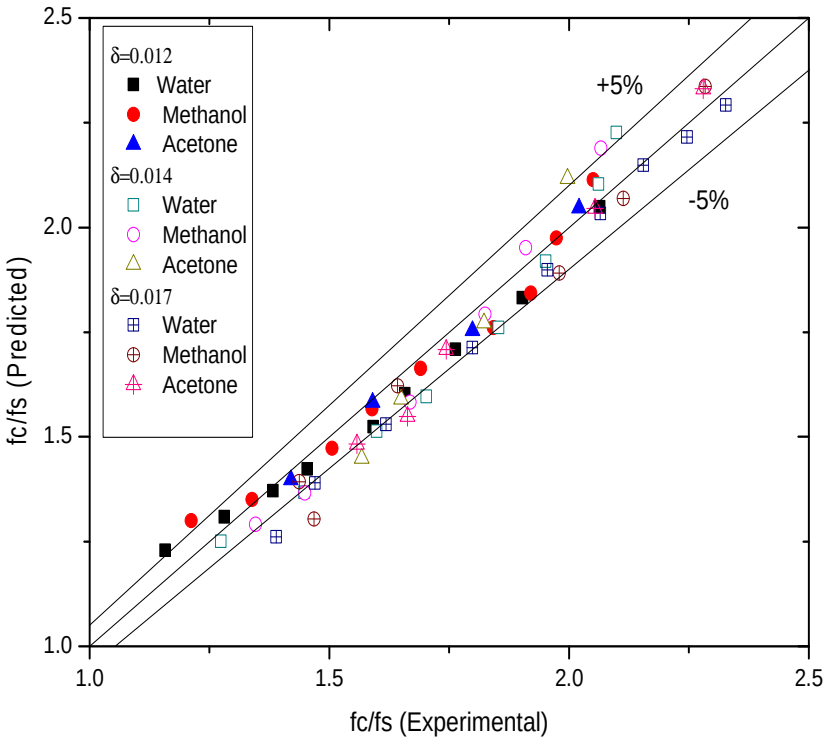

Fig.4.14 Comparison of experimental friction factor ratio (f_c / f_s) with those predicted from present correlation

4.2.6 Comparison with available correlations for friction factor

Let us now examine Figures 4.15 and 4.16 where present experimental data compared with previously developed correlation for laminar flow. Comparison of experimental data with theoretical correlations of Mishra and Gupta (1979) (eqn. 2.3) and Ito (1969) (eqn. 2.1) for laminar flow of Newtonian fluids flowing through helical coils is shown in Figure 4.15, and a summary of percent deviation of predicted values from experimental one is given in Table 4.1.

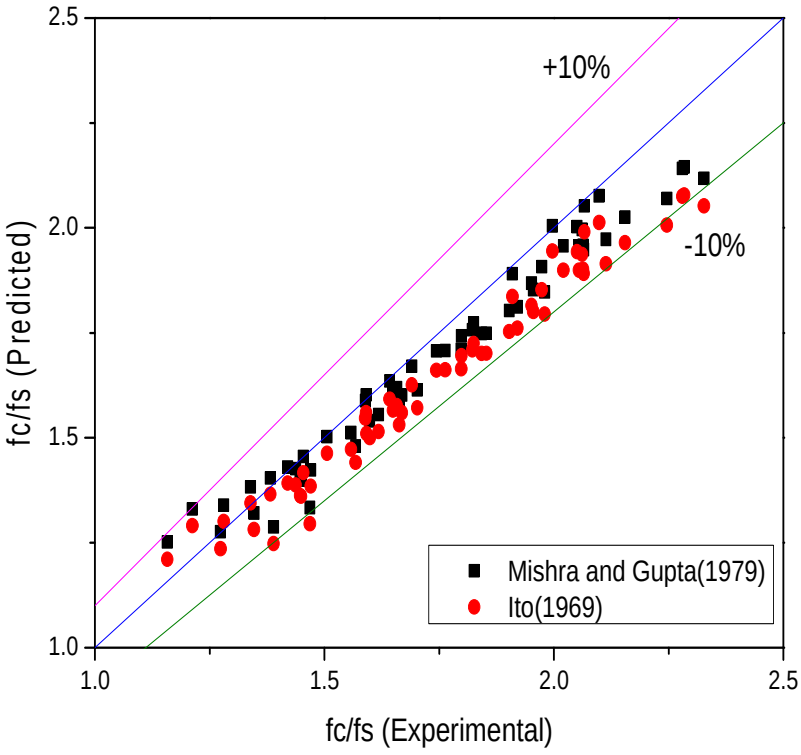

Fig.4.15 Comparison of experimental friction factor ratio (f_c / f_s) with values predicted from correlations of Mishra and Gupta (1979) and Ito (1969)

Predictions from both the correlations are found to be in good agreement within $\pm 10\%$.

Figure 4.16 shows comparison between experimentally obtained friction factor ratio (f_c / f_s) with predicted value using White (1929) (eqn. 2.45) and Mori and Nakayama (1967) (eqn.2.46) correlations. From this figure it is observed that experimental values agree within $\pm 10\%$ from both correlations.

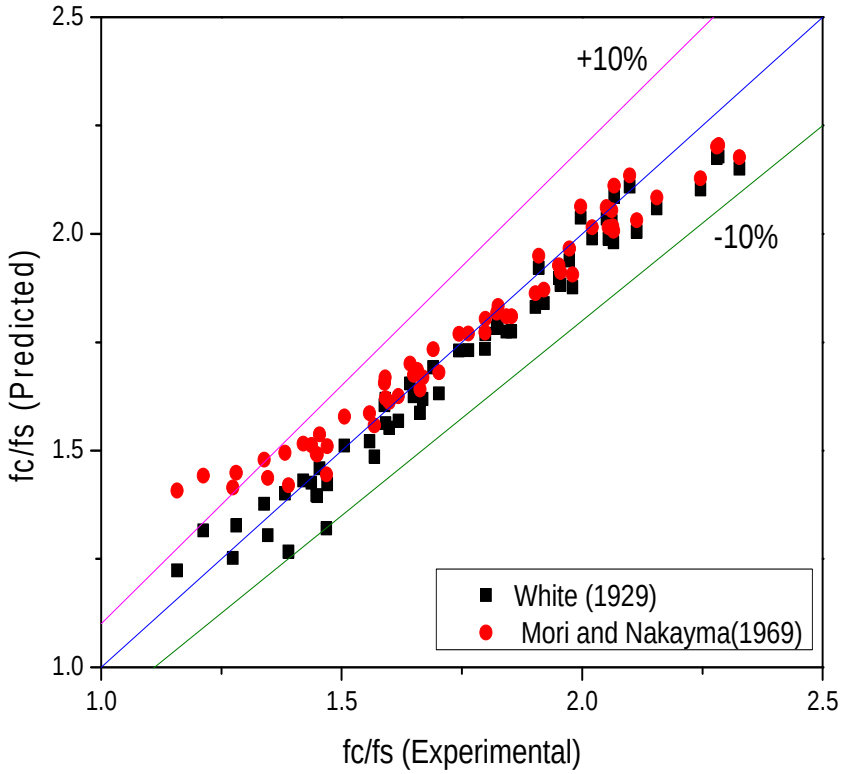

Fig.4.16 Comparison of experimental friction factor ratio (f_c / f_s) with values predicted from correlations of White (1929) and Mori and Nakayama (1967)

Figure 4.17 to 4.19 show the comparison between experimental data of Cioncolini and Santini's (2006) with values predicted by present and those developed by Mishra and Gupta (1979), Ito (1969), White (1929) and Mori and Nakayama (1967) and percent deviation are summarized in Table 4.2.

Comparison between Cioncolini and Santini's (2006) experimental values of f_c / f_s and value predicted from present correlation is shown in Figure 4.17. Present correlation over predicts the experimental values by +10%.

Figure 4.18 shows the comparison between experimental data of Cioncolini and Santini's (2006) with values predicted from correlations of Mishra and Gupta (1979) and Ito (1969). It is observed that both correlations over predict the experimental values by +5%.

Comparison between experimental data of Cioncolini and Santini's (2006) with values obtained from correlations of White (1929) and Mori and Nakayama (1967) is shown in Figure 4.19. Both correlations over predict the experimental values by +10%.

Table 4.1 Percent deviation between present and other correlation for present data

Data	Authors	Correlation	Range	Deviation
Present	Present	$\frac{f_c}{f_s} = 1 + 0.005De$	$\delta = 0.012 - 0.017$ $45 < De < 270$	$\pm 5\%$
	Mishra and Gupta (1979)	$\frac{f_c}{f_s} = 1 + 0.033(\log De)^4$	$\delta = 0.003 - 0.12$ $1 < De < 3000$	$\pm 10\%$
	Ito (1969)	$\frac{f_c}{f_s} = 21.5\left[\frac{De}{(1.56 + \log_{10} De)^{5.}}\right.$	$\delta = 0.015 - 0.61$ $13.5 < De < 2000$	$\pm 10\%$
	White (1929)	$\frac{f_c}{f_s} = \left[\left\{1 - \left(1 - \frac{11.6}{De}\right)^{0.45}\right\}^{2.2}\right]^{-1}$	$11.6 < De < 2000$	$\pm 10\%$
	Mori and Nakayama (1967)	$\frac{f_c}{f_s} = \frac{0.1080\sqrt{De}}{1 - (3.253/\sqrt{De}}$	$13.5 < De < 2000$	$\pm 10\%$

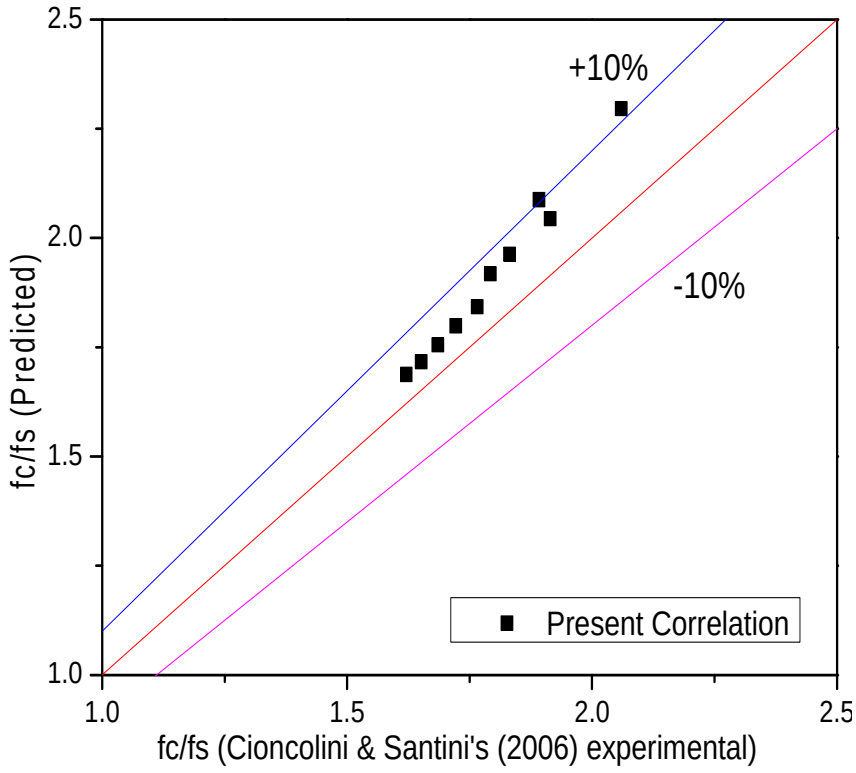

Fig.4.17 Comparison between Cioncolini and Santini's (2006) experimental values of f_c / f_s and values predicted from present correlation

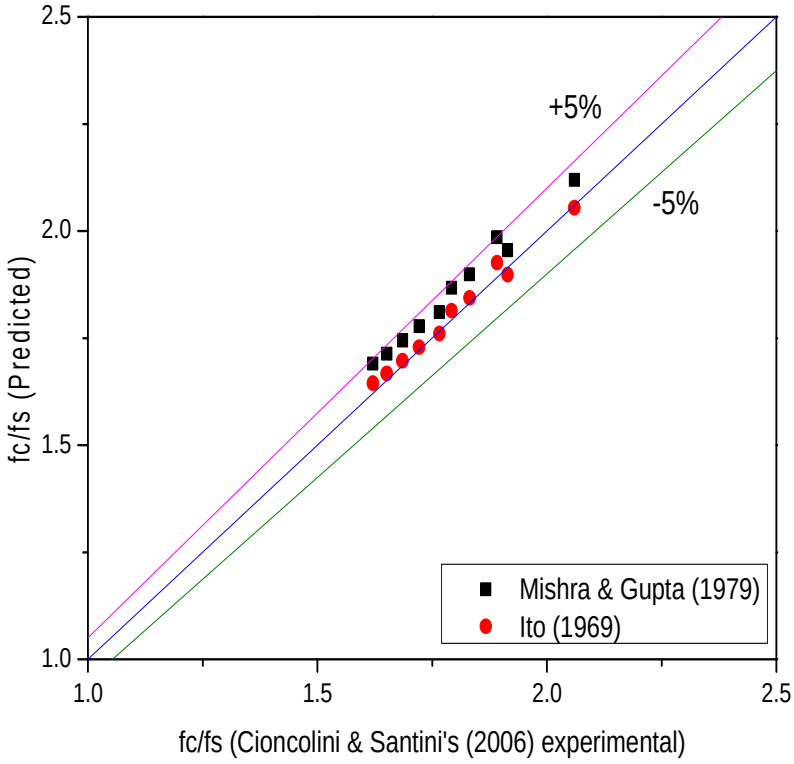

Fig.4.18 Comparison between Cioncolini and Santini's (2006) experimental values of f_c / f_s and values predicted from correlations of Mishra and Gupta (1979) and Ito (1969)

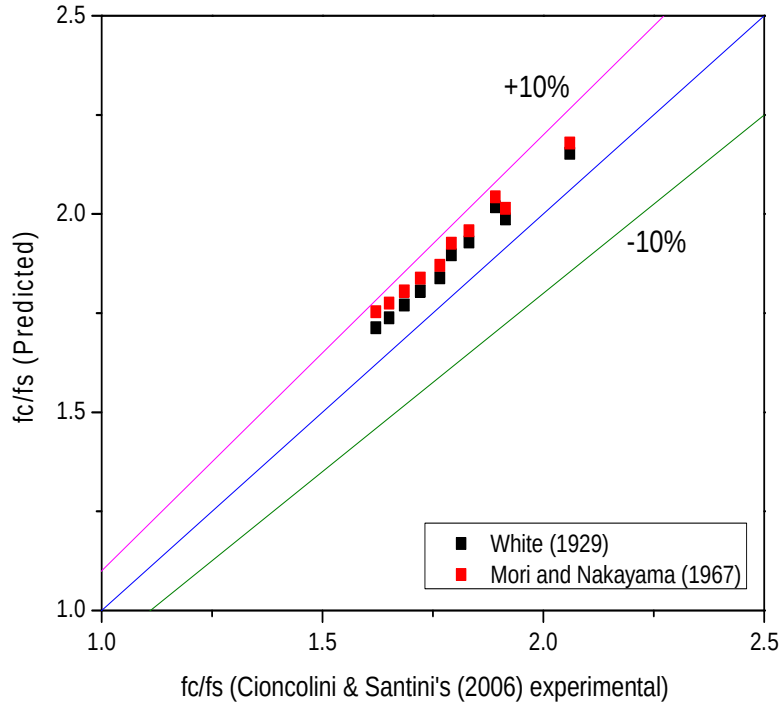

Fig.4.19 Comparison between Cioncolini and Santini's (2006) experimental values of f_c / f_s and values predicted from correlations of White (1934) and Mori and Nakayama (1967)

From above discussions it is clear that Mishra and Gupta (1979) and Ito (1969)'s correlation are better than present correlation for the prediction of Cioncolini and Santini's (2006) experimental data. However prediction from White (1929) and Mori and Nakayama (1967) are same as to those from present correlation.

Table 4.2 Percent deviation between predicted values and experimental data of Cioncolini and Santini's (2006) data

Data	Authors	Correlation	Range	Deviation
Cioncolini and Santini (2006)	Present	$\frac{f_c}{f_s} = 1 + 0.005De$	$\delta = 0.012 - 0.017$ $45 < De < 270$	+10%
	Mishra and Gupta (1979)	$\frac{f_c}{f_s} = 1 + 0.033(\log De)^4$	$\delta = 0.003 - 0.12$ $1 < De < 3000$	+5%
	Ito (1969)	$\frac{f_c}{f_s} = 21.5\left[\frac{De}{(1.56 + \log_{10} De)^{5.73}}\right]$	$\delta = 0.015 - 0.61$ $13.5 < De < 2000$	+5%
	White (1929)	$\frac{f_c}{f_s} = \left[\left\{1 - \left(1 - \frac{11.6}{De}\right)^{0.45}\right\}^{2.2}\right]^{-1}$	$11.6 < De < 2000$	+10%
	Mori and Nakayama (1967)	$\frac{f_c}{f_s} = \frac{0.1080\sqrt{De}}{1 - (3.253/\sqrt{De}}$	$13.5 < De < 2000$	+10%

4.2.7 Generalized correlation for friction factor

Based on present and Cioncolini and Santini's (2006) experiential data for laminar flow in helical coil using least squares regression following generalized correlation is developed.

$$\frac{f_c}{f_s} = 1 + 0.008\ De^{\,0.897} \tag{4.2}$$

The above correlation correlates the both sets of data with standard deviation of $\pm 8\%$. Figure 4.20 shows comparison of the experimental f_c / f_s ratio with predicted from the generalized correlation. From this figure it is observed that all data lie within $\pm 8\%$ band.

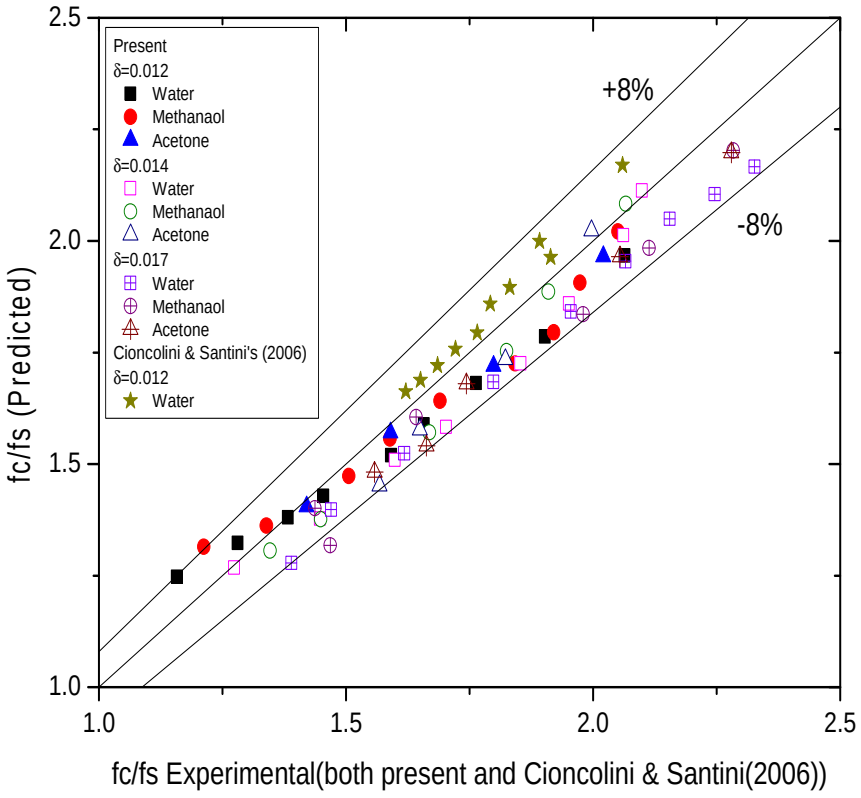

Fig.4.20 Comparison of experimental friction factor ratio (f_c / f_s) (both present Cioncolini and Santini's (2006)) and with those predicted from the generalized correlation

4.3 Heat transfer characteristics

Heat transfer results in a helical coil with micro-diameter tube for laminar flow under constant heat flux conditions are presented in this section. Based on the present experimental results and those available in published literature a suitable dimensionless correlation for the prediction of heat transfer coefficient is also presented.

4.3.1 Variation of heat transfer coefficient with flow rate

Experiments were performed for measuring heat transfer during single phase laminar flow in a helical coil. Effect of flow rate on average heat transfer coefficient in a helical coil with inner diameter of 720 μm was investigated. These results are shown as $\bar{h}$ vs u plots in Figures 4.21 for all three fluids. The basic heat transfer data of helical coil with micro-diameter tube for all working fluids used are presented in Table D.5. The heat flux was varied from 1760-28233 W/m^2. An increasing trend in the average heat coefficient is observed with increasing flow velocity. The trend

shown by *h vs. u* plot is similar to that reported by previous workers (Kumar et al. (2006), Wongwises and Polsongkram (2006), Jamshidi et al. (2013), Kahani et al. (2013) etc.). The average heat transfer coefficient has ranged from 1096 to 6012 W/m^{2}K for water, 344 to 1785 W/m^{2}K for methanol and 284 to 815 W/m^{2}K for acetone. Heat transfer coefficient in water is much greater than that for methanol and acetone due to its better thermal properties. Methanol offer greater heat transfer coefficient than acetone. From thermal point of view water is more suitable because it offers better heat transfer coefficient than methanol and acetone.

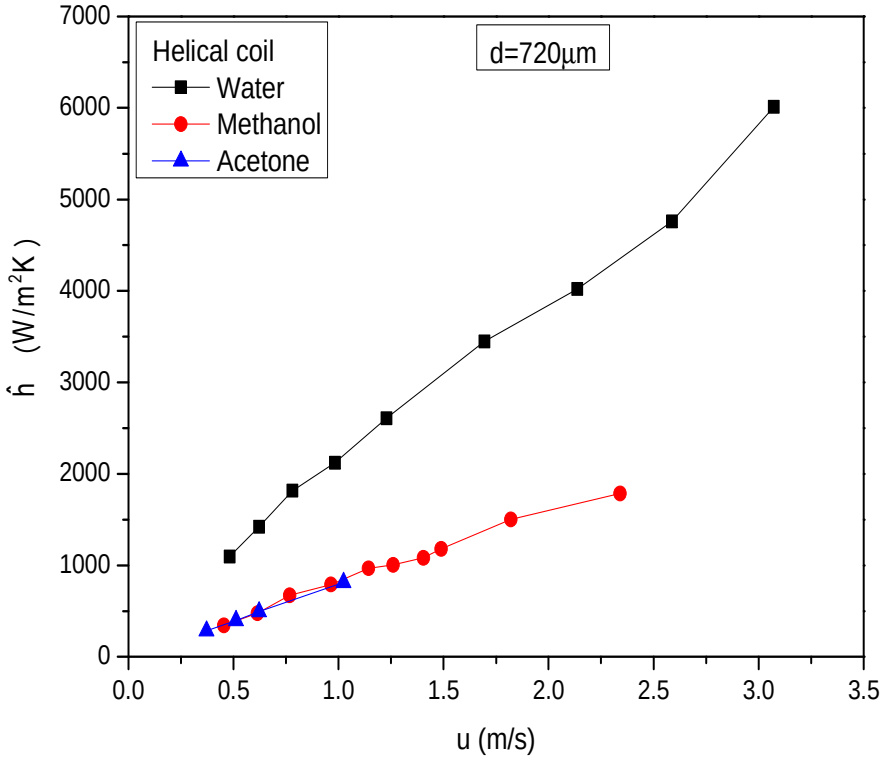

Fig.4.21 Average heat transfer coefficient vs. velocity in a helical coil for all three fluids

4.3.2 Variation of wall temperature in a helical coil

The variation of average wall temperature with velocity in a helical coil for all working fluids under constant heat flux conditions 1760-28233 W/m^2 is shown in Figure 4.22. It is noticeable that wall temperature decreases as velocity of fluid increases. The average wall temperature has varied from 354 to 310 K for water, 323 to 306 K for methanol and 314 to 307 K for acetone. In all cases an exponential decrease in wall temperature has been noticed.

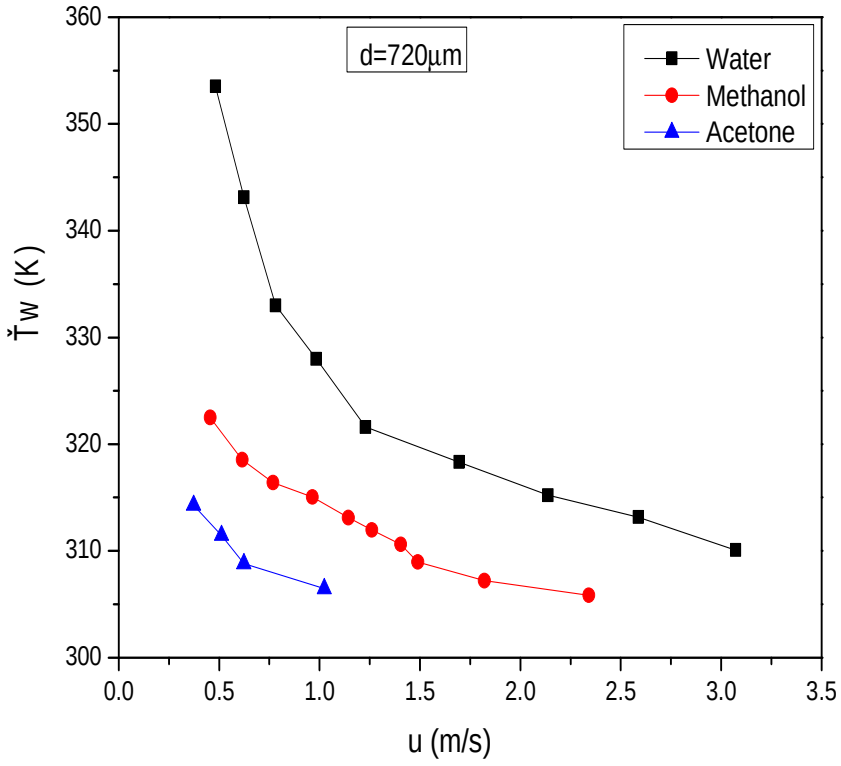

Fig.4.22 Variation of average wall temperature with velocity in a helical coil

4.3.3 Variation of bulk fluid temperature in a helical coil

The variation of bulk fluid temperature along the helical coil is shown in Figure 4.23 for all three working fluids. The bulk temperature has varied from 327 to 306 K for water, 310 to 304 K for methanol and 308 to 305 K for acetone. The bulk fluid temperature decreases as the velocity increases. The trend is similar to that shown by the average tube wall temperature.

4.3.4 Variation of Nusselt number with Reynolds number in a helical coil

Nusselt number in a helical coil with micro-diameter tube of curvature ratio 0.012 for all working fluids is presented in Figure 4.24. The Reynolds number has varied from 447 to 2083. The difference between Nusselt number for water and methanol is less due to similar Prandtl number range, whereas Nusselt number for acetone lies below water and methanol due its lower Prandtl number. It is noticeable that as the Reynolds number increases Nusselt number increases linearly on log Nu vs. log Re plot.

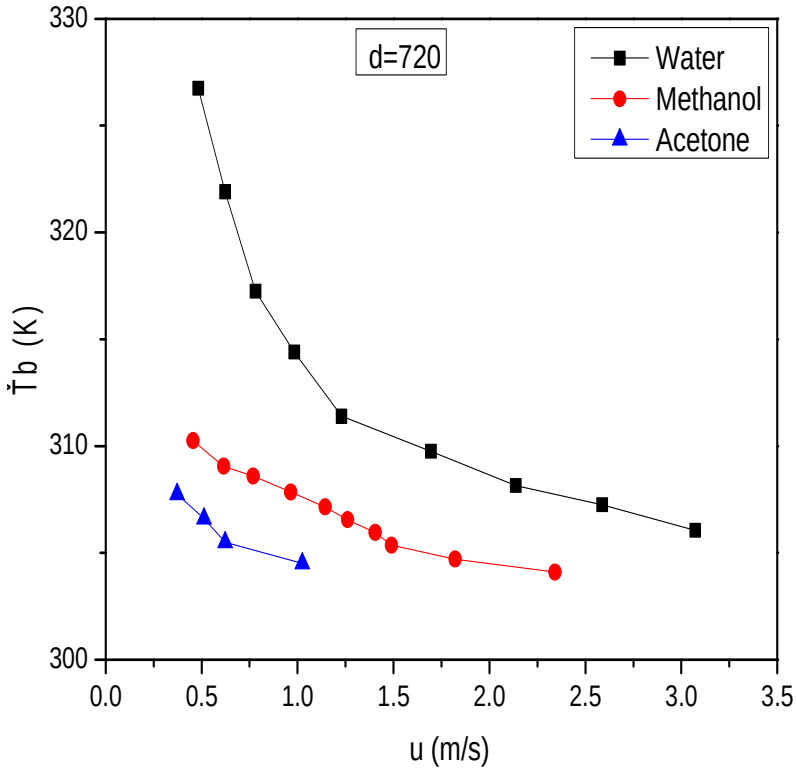

Fig.4.23 Variation of bulk fluid temperature with velocity in a helical coil

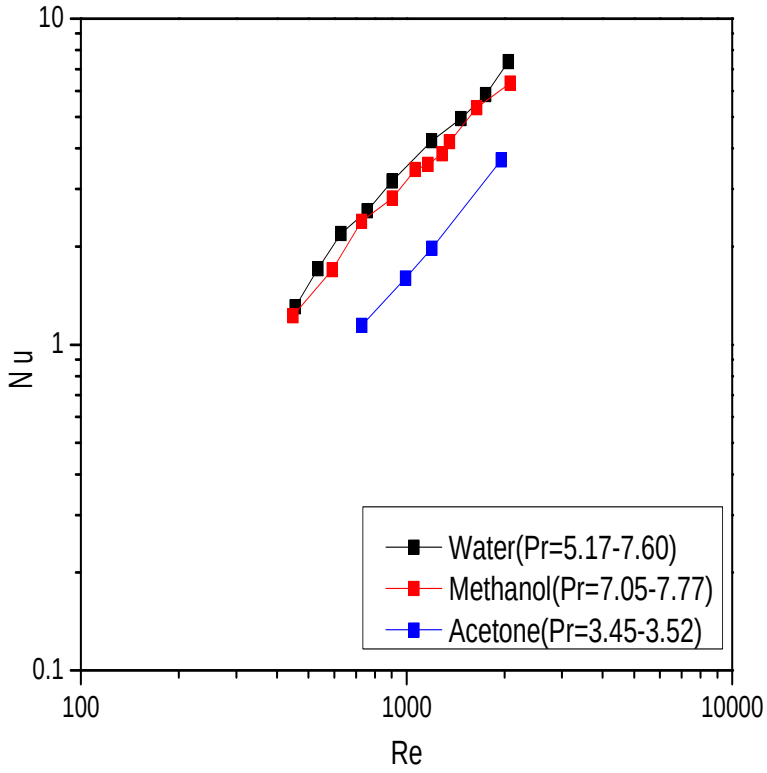

Fig.4.24 Nusselt number in a helical coil of curvature ratio 0.012 for three working fluids

Present and Kahani et al.'s (2013) experimental Nusselt number data for helical coil is shown in Figure 4.25 as Nu versus Re plot. Kahani et al.'s (2013) generated heat transfer data (given in Table D.16) for helical coil of d=7 mm, D=70-140 mm, p=24-42 mm, L=1318.8 mm and N=3-6 using water and alumina nano-suspension of different concentrations in water as working fluids. Prandtl number varied from 5.89 to 8.87. It must be mentioned here that the dimension of coil and tube used by Kahani et al. (2013) are much larger than those used within present work. From Figure 4.38 it is seen that the trend of Nu-Re plot for present and Kahani et al.'s (2013) is similar. Thus it may be possible to develop generalized correlation for a wide range of working fluids. From this figure it is also observed that as concentration of nanofluids increases Nusselt number increases.

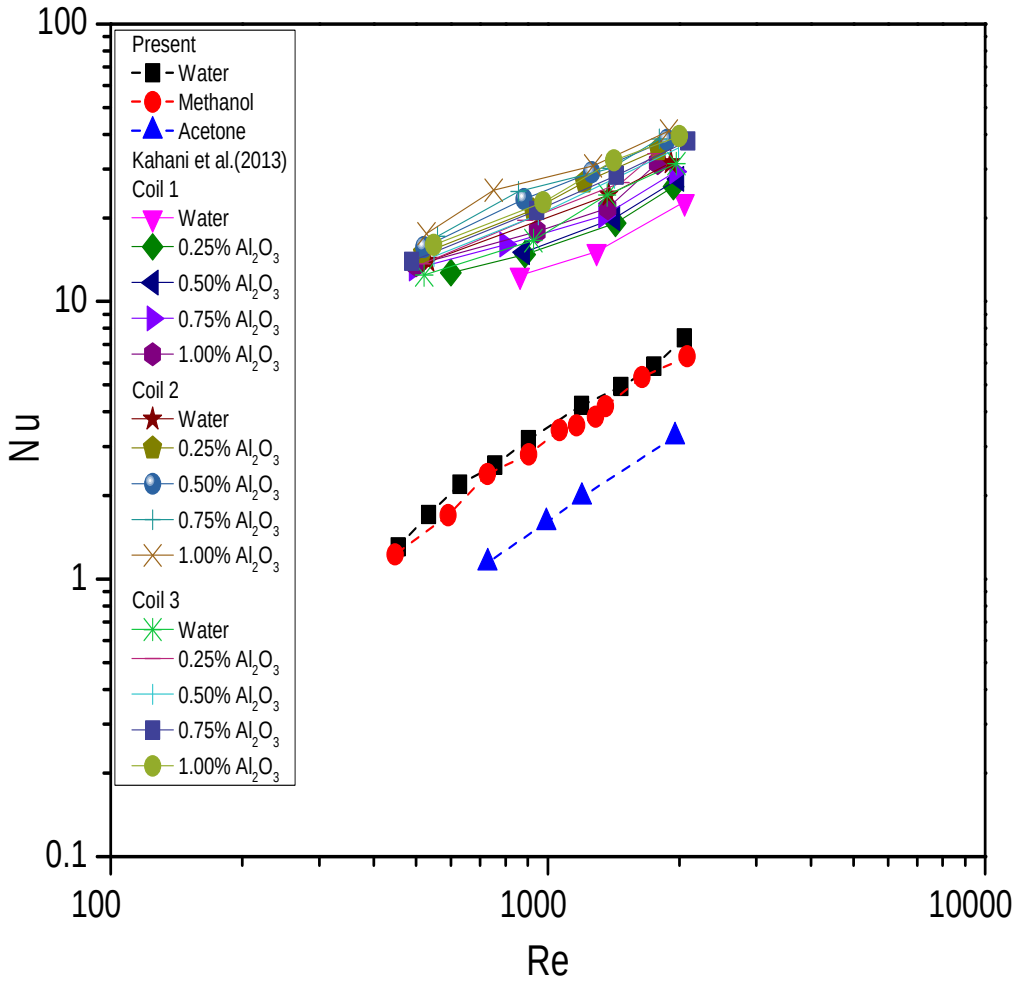

Fig.4.25 Nu vs. Re plot: Present and Kahani et al.'s (2013) experimental Nusselt number in helical coils

4.3.5 Variation of Nusselt number with Dean number in a helical coil

Variation of Nusselt number with Dean number in a helical coil of curvature ratio 0.012 for all working fluids is presented in Figure 4.26. The Dean number varied from 49 to 228. From this figure it is seen that as the Dean number increases Nusselt number also increases.

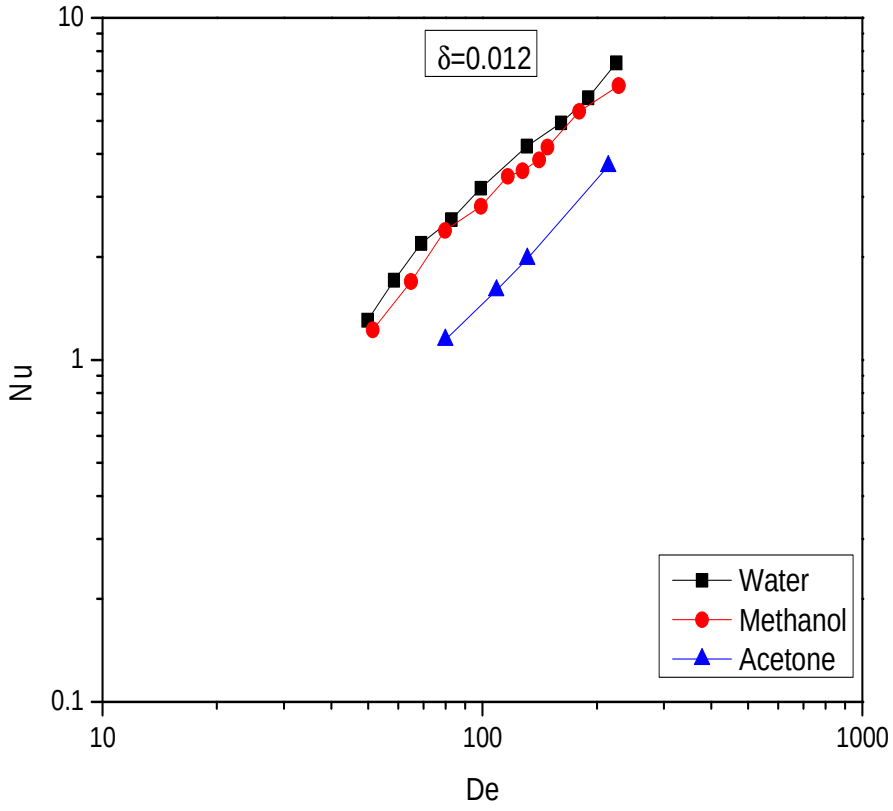

Fig.4.26 Variation of Nusselt number with Dean number in a helical coil of curvature ratio 0.012

4.3.6 Correlation for heat transfer

Using the Nusselt number-Reynolds number data of a helical coil with micro-diameter tube of curvature ratio 0.012 having constant coil diameter and pitch generated in the present study, the least squares regression analysis indicated that

$$Nu = 0.008De^{0.949}\,\mathrm{Pr}^{0.75} \tag{4.3}$$

correlates the present results quite well. The above correlation is valid for $\delta = 0.012$, De = 49-228 and Pr=3.5-7.8 and predicts the present data with a standard deviation of ± 6 %.

The parity plot of Nusselt number predicted from the present correlation and experimentally obtained Nusselt number is shown in Figure 4.27. It is seen that all the Nusselt number values lie within ± 6 % range.

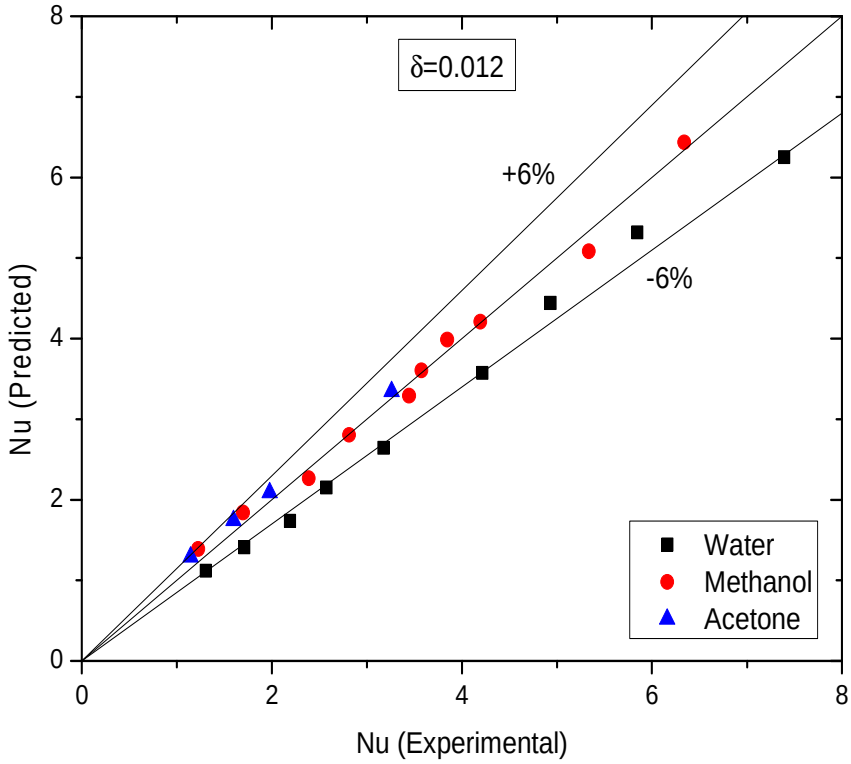

Fig.4.27 Predicted Nusselt number from present correlation vs. experimentally obtained Nusselt number

4.3.7 Comparison with other available correlations for heat transfer

A comparison between experimental Nusselt number and value predicted from Kalb and Seider (1974) (eqn. 2.52) and Dravid et al. (1971) (eqn. 2.62) for laminar flow of Newtonian fluids flowing through helical coil is presented in Figure 4.28 and a summary of percent deviation of predicted values from experimental one is given in Table 4.3. Both correlations are found to predict +30% higher values. Thus it is clearly seen that for smaller curvature ratio ($\delta = 0.012$) used in the present work these correlation over predict the Nusselt number values. Kalb and Sieder's (1974) correlation was developed for $0.01 < d/D < 0.1$, $80 < De < 1200$ and $0.7 < \mathrm{Pr} < 5$. Dravid et al.'s (1971) correlation was developed for a curvature ratio of 0.0536 for laminar regime $50 < De < 2000$ and $5 < \mathrm{Pr} < 175$. These differences in the range of operating parameters are likely to influence the validity of developed correlation over a different range of operating parameters.

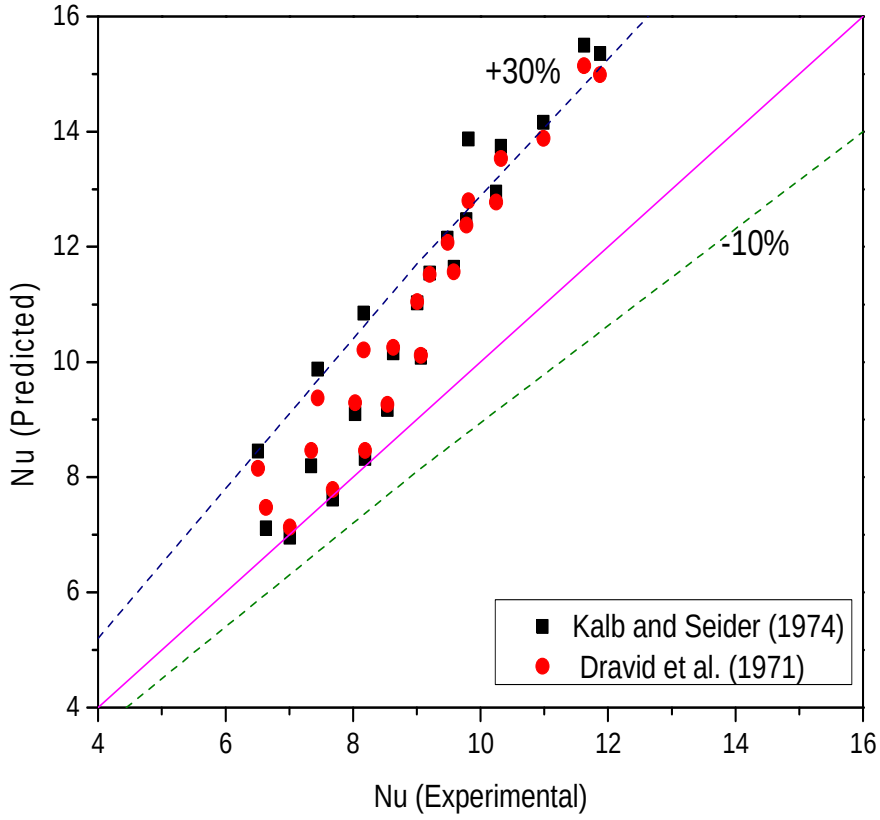

Fig.4.28 Comparison of experimental Nusselt number with value predicted from correlations of Kalb and Seider (1974) and Dravid et al. (1971)

Table 4.3 Percent deviation between present correlation and other for the present data

Data	Authors	Correlation	Range	Deviation
Present	Present	$Nu = 0.008De^{0.949}\,\mathrm{Pr}^{0.75}$	$\delta = 0.012$, $49 < De < 228$ $\mathrm{Pr} = 3.5 - 7.8$	± 6 %
	Kalb and Seider (1974)	$Nu = 0.836De^{0.5}\,\mathrm{Pr}^{0.1}$	$0.01 < d/D < 0.1$ $80 < De < 1200$ $0.7 < \mathrm{Pr} < 5$.	+30%
	Dravid et al. (1971)	$Nu = \left[0.76 + 0.65\sqrt{De}\right]\mathrm{Pr}^{0.175}$	$\delta = 0.0536$ $50 < De < 2000$ $5 < \mathrm{Pr} < 175$	+30%

Figure 4.29 and 4.30 shows the comparison between experimental data of Kahani et al.'s (2013) and values predicted from present correlation and correlations of Kalb and Seider (1974) and Dravid et al. (1971). Comparison between Kahani et al.'s (2013) experimental results with value predicted from present correlation is shown in Figure 4.29. Figure shows present correlation under predicts the experimental values by as much -62 %. Curvature ratio of helical coil used by Kahani et al.'s (2013) was 0.05 to 0.1 which is much higher than that used in the present work ($\delta = 0.012$).

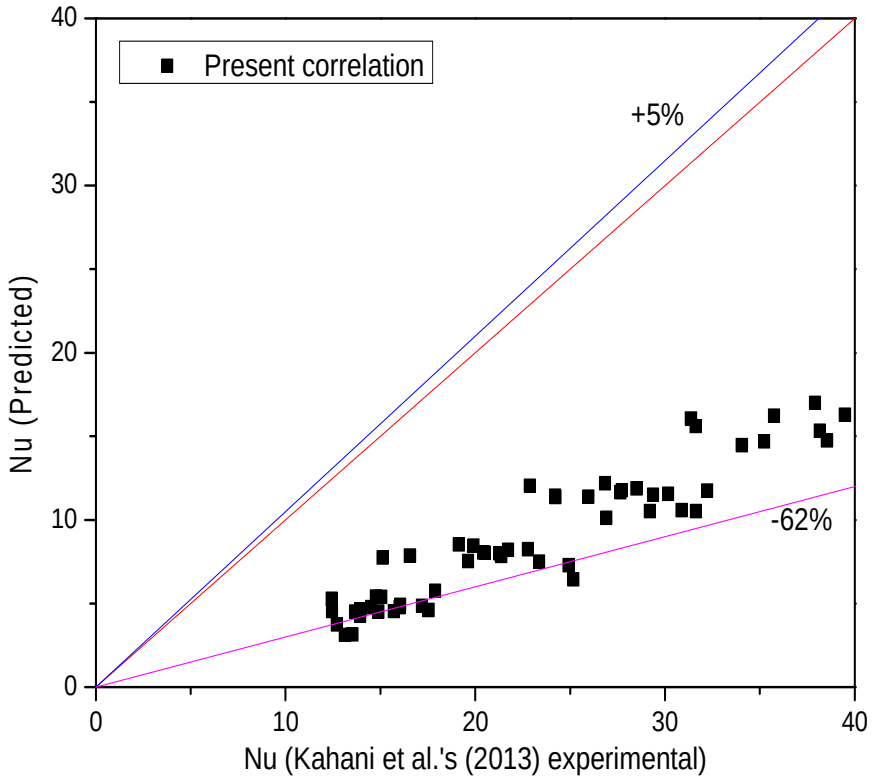

Fig.4.29 Comparison between Kahani et al.'s (2013) experimental results with values predicted from present correlation

Comparison between Kahani et al.'s (2013) experimental results with values predicted from correlations of Kalb and Seider (1974) and Dravid et al. (1971) is shown in Figure 4.30, and percent deviation values are summarized in Table 4.4. It is seen that most are under predicted and lie within -40%.

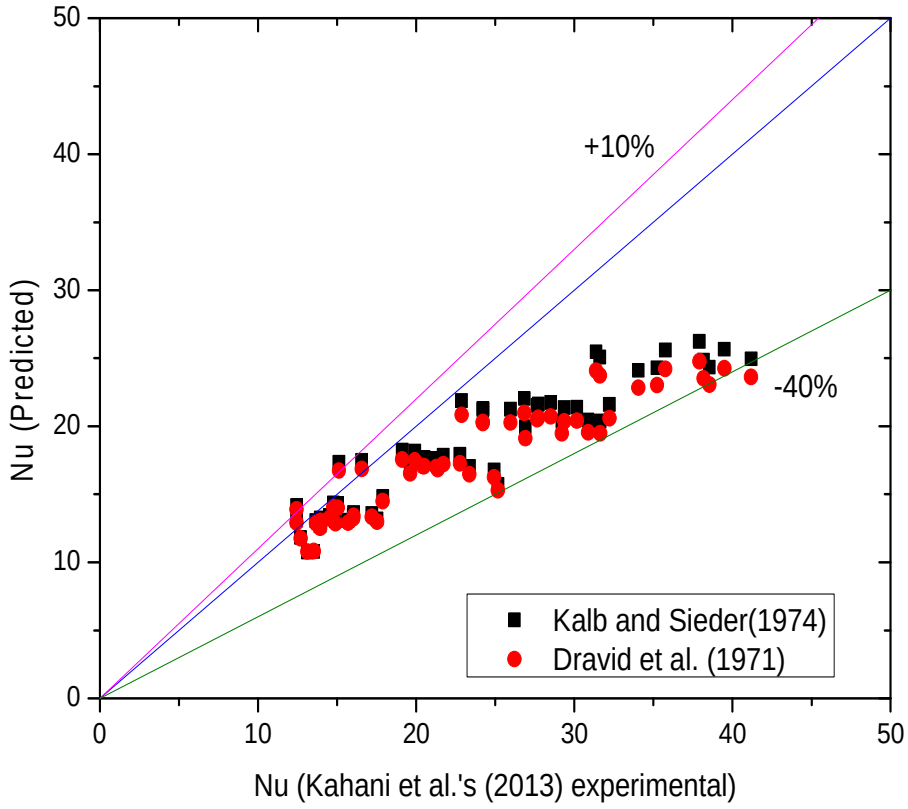

Fig.4.30 Comparison between Kahani et al.'s (2013) experimental results with values predicted from Kalb and Seider's (1974) and Dravid et al.'s (1971) correlations

Table 4.4 Percent deviation between predicted values and experimental data of Kahani et al.'s (2013)

Data	Authors	Correlation	Range	Deviation
Kahani et. al. (2013)	Present	$Nu = 0.008De^{0.949}\,\mathrm{Pr}^{0.75}$	$\delta = 0.012$, $49 < De < 228$ $\mathrm{Pr} = 3.5 - 7.8$	-62%
	Kalb and Seider (1974)	$Nu = 0.836De^{0.5}\,\mathrm{Pr}^{0.1}$	$0.01 < d/D < 0.1$ $80 < De < 1200$ $0.7 < \mathrm{Pr} < 5$.	-40%
	Dravid et al. (1971)	$Nu = \left[0.76 + 0.65\sqrt{De}\right]\mathrm{Pr}^{0.1}$	$\delta = 0.0536$ $50 < De < 2000$ $5 < \mathrm{Pr} < 175$	-40%

`

4.3.8 Generalized correlation for heat transfer

In view of the large deviation between predicted and available experimental values an effort was made to develop a generalized correlation using Kahani et al. (2013) and present data for laminar flow in helical coils. Using the least squares regression analysis can be written

$$Nu = 0.002\, De^{1.2621}\, \mathrm{Pr}^{0.89} \tag{4.4}$$

satisfactorily correlates the entire laminar regime data. The above correlation valid for $\delta = 0.012$ -0.1, De=49-631 and Pr=3.5-7.38 and correlates both sets of data with a standard deviation of $\pm 18\%$.

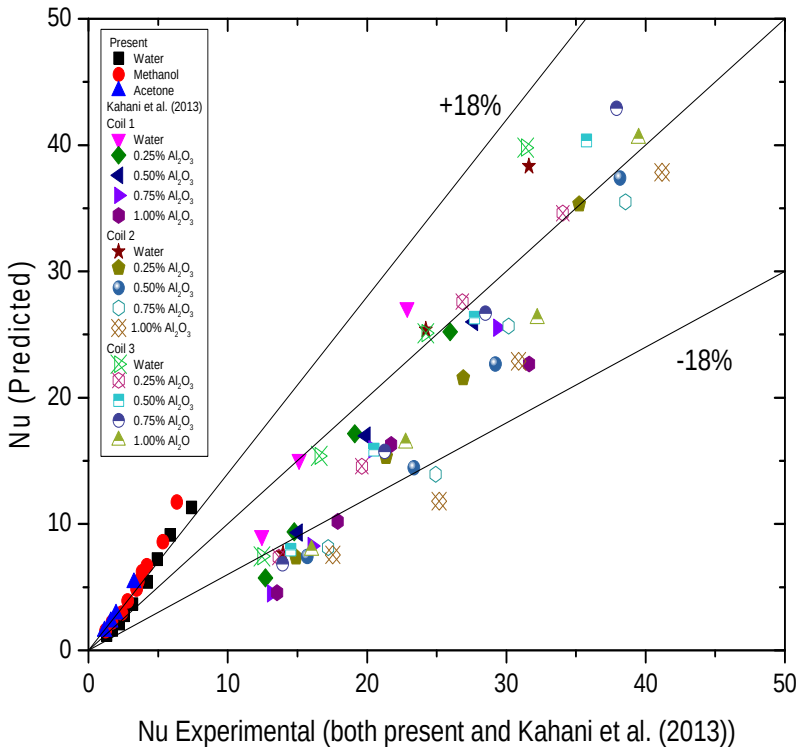

Fig.4.31 Comparison of experimental Nusselt number (both present and Kahani et al. (2013)) with those predicted from the generalized correlation

Figure 4.31 show the parity plot between experimental Nusselt number (both present and Kahani et al. (2013)) and those predicted from the generalized correlation. It is seen that most of the data lie within the $\pm 18\%$ band.